Defect-dependent carrier transport behavior of polymer:ZnO composites/electrodeposited CdS/indium tin oxide devices

Yow-Jon Lin (林祐仲)[a] and C. F. You
Institute of Photonics, National Changhua University of Education, Changhua 500, Taiwan

(Received 5 March 2015; accepted 16 July 2015; published online 28 July 2015)

Currents through the poly(3,4-ethylenedioxythiophene) doped with poly(styrenesulfonate) and ZnO nanoparticles (PEDOT:PSS:ZnO)/CdS/indium tin oxide (ITO) hetero-structures are studied. The authors introduced the electrodeposition technique with sulfide treatment to improve the film quality of CdS. It is shown that sulfide treatment leads to a reduction in the number of donor-like defects (that is, sulfur vacancies and cadmium interstitials) in the CdS films, which leads to the conversion of carrier transport behavior from Poole-Frenkel emission to thermionic emission-diffusion for PEDOT:PSS:ZnO/CdS/ITO devices. A correlation is identified for providing a guide to control the current transport behavior of PEDOT:PSS:ZnO/CdS/ITO devices. © *2015 AIP Publishing LLC*.
[http://dx.doi.org/10.1063/1.4927520]

I. INTRODUCTION

Cadmium sulfide (CdS), a member of II-VI semiconducting compounds, is of considerable interest. CdS with medium band gap (2.42–2.62 eV), high absorption coefficient (10^4–10^5 cm^{-1}), and high mobility (440 cm^2 V^{-1} s^{-1}) is a well-known and common n-type heterojunction partner in thin film chalcogenide solar cells.[1–5] A wide variety of techniques have been employed for the deposition of CdS thin films.[6–11] Recently, organic/inorganic semiconductor hetero-structures have attracted much attention because of their potential application as optoelectronic and electronic devices.[12–16] Here, we introduce the electrodeposition technique to grow the CdS films[17,18] and fabricated the poly(3,4-ethylenedioxythiophene) doped with poly(styrenesulfonate) and ZnO nanoparticles (PEDOT:PSS:ZnO)/CdS/indium tin oxide (ITO) devices. CdS nanocrystalline thin films belonging to the cadmium chalcogenide family and because of its suitable band gap and stability (with hexagonal structure) is highly favorable for solar cell application as a window layer material for CdS/CdTe heterojunction solar cells.[19,20] The synthesis and characterization of CdS are of significant interest for both fundamental and applied research, due to their tunable electronic and optical properties arising from the stoichiometry effect.[21,22] Therefore, it is necessary to improve the disadvantages through various thermal treatments. However, thermal annealing with $CdCl_2$ could make some of sulfur evaporation.[23,24] We introduce the electrodeposition technique with sulfide treatment to improve the film quality of CdS. In this study, we present results about the influence of sulfide treatment on the defects in the CdS layer and the conduction mechanism of PEDOT:PSS:ZnO/CdS/ITO devices. It is found that the conversion of carrier transport behavior from Poole-Frenkel (PF) emission to thermionic emission (TE)-diffusion for PEDOT:PSS:ZnO/CdS/ITO devices, which is the result of a reduction in the number of donor-like defects in the CdS films. Knowledge of the carrier transport behavior and defects inside CdS films are helpful for device performance improvement.

II. EXPERIMENTAL PROCEDURE

ITO was deposited onto the glass surface by electron-beam evaporation. An oxidized target of In_2O_3 and SnO_2 with a weight proportion of 9:1 was used in conjunction with O_2 (8 SCCM) gas as an ambient gas for ITO deposition. The working pressure was 8×10^{-3} Pa. The substrate temperature was fixed at 300 °C. The film thickness of ITO is 100 nm. ITO/glass with a sheet resistance of 55 Ω/sq was cleaned in an ultrasonic bath of acetone and methanol. The CdS deposition was carried out in an aqueous bath prepared by dissolution in deionized water of analytical grade reagents of $CdCl_2$ (0.1 M) and $Na_2S_2O_3$ (0.03 M). Hydrochloric acid was added to reach the desired pH = 2.0.[7] The solution was magnetically stirred during deposition. The electrodeposition cell was a glass vessel with a three-electrode systems consisting of an Ag/AgCl reference electrode, a Pt sheet counter electrode, and an ITO/glass working electrode. The CdS electrodeposition was carried out using a computer controlled potentiostat (Jiehan, ECW-5000 electrochemical workstation). All the cathodic voltages reported here were applied with respect to the reference electrode. Alternatively, electrodeposition in aqueous solution was carried out by the cathodic deposition at a potential of −0.7 V versus Ag/AgCl reference electrode. The grown time and temperature were 30 min and 80 °C, respectively. The film thickness of CdS, as estimated from field emission scanning electron microscopy, was 70 nm. To deoxygenate the electrolyte solution, nitrogen gas was bubbled before and during the deposition. The CdS films were then inserted into a furnace and annealed at 500 °C for 1 h in pure nitrogen ambient.[20] Then, some of CdS samples were dipped into a 60 °C yellow $(NH_4)_2S_x$ solution (with 6% S, Nippon Shiyaku Co., Ltd.) for 45 min (referred to as sulfide-treated CdS samples).[25] The surface morphology of CdS was studied using atomic force

[a]Author to whom correspondence should be addressed. Electronic mail: rzr2390@yahoo.com.tw

 © 2015 AIP Publishing LLC

Reuse of AIP Publishing content is subject to the terms at: https://publishing.aip.org/authors/rights-and-permissions. Download to IP: 91.202.128.12 On: Thu, 23 Jun 2016 05:14:59

microscopy (AFM). Using a He–Cd laser (325 nm) as an excitation source, the photoluminescence (PL) spectra were observed for CdS samples at 300 K. Photoelectrochemical measurement was carried out in a solution containing 0.35 M Na_2SO_3 and 0.24 M Na_2S (pH = 12.8). The solution was purged by nitrogen to remove the dissolved oxygen before the experiment. The working electrode (CdS/ITO) had a surface area of 1.0 cm^2, and a Pt sheet and a saturated Ag/AgCl electrode were used as the counter and reference electrodes, respectively. The photocurrent was measured under AM 1.5 G condition with an illumination intensity of 100 mW/cm^2 using a solar simulator. On the other hand, the average size of the ZnO nanoparticles purchased from Centron Biochemistry Technology Co., Ltd. was 35 nm. PEDOT:PSS (Clevios P VP. AI 4083) was purchased from Heraeus. ZnO (40 mg) was dispersed in methanol (2.5 ml), followed by ultrasonication for 60 min to improve the dispersion of ZnO nanoparticles. Composite samples were prepared by adding PEDOT:PSS (20 ml) to ZnO solutions (referred to as PEDOT:PSS:ZnO), followed by ultrasonication for 60 min. Then, PEDOT:PSS:ZnO was deposited on CdS surfaces by spin coating. Spin casting was performed at 2000 rpm for 60 s per cast layer. After depositing by spin coating, the films were baked at 150 °C for 30 min on a hotplate. The procedures from coating to drying were repeated five times. Au electrode deposited onto the PEDOT:PS:ZnO surface was produced using shadow masking through sputter coater (SC5750). According to a previously reported result,[15] we found that the incorporation of ZnO nanoparticles leads to changes in the chemical structure of PEDOT:PSS from a mixture of benzoid and quinoid to mostly quinoid, increasing the electrical conductivity. For PEDOT:PSS:ZnO/CdS/ITO devices, the current-voltage (I-V) curve was measured using a Keithley Model-4200-SCS semiconductor characterization system. The I–V characteristics were measured in the temperature range from 280 to 300 K in steps of 10 K using a temperature controlled cryostat.

III. RESULTS AND DISCUSSION

Figure 1 shows the I-V characteristics of the PEDOT:PSS:ZnO/CdS/ITO and PEDOT:PSS:ZnO/sulfide-treated CdS/ITO devices at 300 K in the dark, respectively. The ratio of the forward to reverse current at a bias voltage of ±1 V for the PEDOT:PSS:ZnO/CdS/ITO (PEDOT:PSS:ZnO/sulfide-treated CdS/ITO) device was calculated to be 39 (274). A good rectification behavior is found for PEDOT:PSS:ZnO/sulfide-treated CdS/ITO devices. The forward I-V characteristics as shown in Fig. 1 can be classified into two regions according to the applied voltages. In the voltage region of 0.8–2.0 V, the forward current deviates from linearity due to the effect of a series resistance on the PEDOT:PSS:ZnO/CdS/ITO (PEDOT:PSS:ZnO/sulfide-treated CdS/ITO) structure. In the voltage region of 0.0–0.8 V, the forward current was tentatively analyzed by using a simple Schottky model. In this model, the carrier transport occurs across the barrier by TE, the drift and diffusion of carriers within the depletion region are less important. The current as a function of applied biasing voltages is given by[26,27]

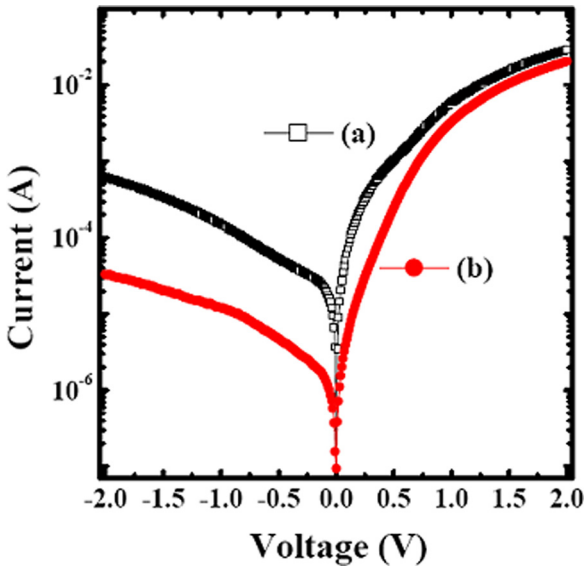

FIG. 1. I-V characteristics of the (a) PEDOT:PSS:ZnO/CdS/ITO and (b) PEDOT:PSS:ZnO/sulfide-treated CdS/ITO devices observed at 300 K in the dark.

$$I = I_o\left[\exp\left(\frac{qV}{\eta kT}\right) - 1\right], \tag{1}$$

where I_o is the reverse saturation current, q is the elementary charge, η is the ideality factor, T is the measurement temperature, and k is the Boltzmann constant. The PEDOT:PSS:ZnO/CdS/ITO and PEDOT:PSS:ZnO/sulfide-treated CdS/ITO devices exhibit the large η ($\eta > 6$), indicating that the forward current cannot be explained by the TE theory. The derived value of η value is larger than unity, indicating that there is a deviation from the ideality behavior. The deviation may be attributed to either the recombination of electrons and holes in the depletion region, current mechanism, presence of a large number of surface states, and/or increase of diffusion current.[28–30] Another possibility may be the transport mechanism in these devices which is not purely due to TE. With consideration that the CdS layers without sulfide treatment had a high trap density, the PF emission may be the possible phenomenon that explains the deviation from the ideality of the PEDOT:PSS:ZnO/CdS/ITO device. These traps may originate from the formation of the large number of donor-like defects [that is, sulfur vacancies (V_S) and cadmium interstitials (Cd_i)] in the CdS film.[31,32] Based on the PF emission, the I-V relationship is given as follows:[33,34]

$$I = \frac{S_a C_P V}{d}\exp\left[\frac{-q\left(\phi_T - \sqrt{\frac{qV}{\pi\varepsilon_r\varepsilon_o d}}\right)}{kT}\right], \tag{2}$$

where $q\phi_T$ is the trap energy level in the CdS film, d is the thickness of the CdS layer, ε_o is the vacuum dielectric constant, ε_r is the value of the dielectric permittivity, S_a is the contact area, and C_P is the preexponential factor. PF emission is a field-assisted thermal de-trapping of a carrier from the bulk material into the conduction band [path (2) in Fig. 1 shown in Ref. 34].

Reuse of AIP Publishing content is subject to the terms at: https://publishing.aip.org/authors/rights-and-permissions. Download to IP: 91.202.128.12 On: Thu, 23 Jun 2016 05:14:59

The experimental results fit the PF emission theory very well for PEDOT:PSS:ZnO/CdS/ITO devices (Fig. 2), suggesting the dominant transport property is the PF emission. The derived value ($\sim$10) of ε_r is larger than the reported values varied in the range from 4 to 7 and smaller than the reported value (11.6).[35,36] In addition, $q\phi_T$ in the CdS film is derived to be about 0.2 eV, which is consistent with the reported values.[37,38] According to the previously reported experimental results,[39–41] we found that the energy level of V_S is located at about 0.6 eV below the conduction-band edge (E_C) and the energy level of Cd_i is located at about 0.2 eV below E_C. This result implies that the existence of the large number of Cd_i in the CdS layer leads to the dominance of PF emission for PEDOT:PSS:ZnO/CdS/ITO devices. The PF effect was prevalent for charge transport in the Langmuir-Blodgett films containing CdS nanoparticles and CdS particles acted as electron traps in the bulk of the composite films.[37] Senthilarasu *et al*. found that the electrical conduction mechanism prevailing in the Zinc-phthalocyanine/CdS junctions is of PF type.[42] For CdS/Si multi-interface nanoheterojunctions, the forward electrical behavior was found to be highly related to the distribution of interfacial trap states and the existence of localized electric field.[43] Based on the previously reported results,[18,44–46] it is found that the work function of ITO (PEDOT:PSS) is 4.7 (5.1) eV, the band gap of CdS is 2.45 eV, and the electron affinity of CdS is 4.5 eV. The energy band diagram of the structure is given in Fig. 3.

On the other hand, for PEDOT:PSS:ZnO/sulfide-treated CdS/ITO devices, the experimental results cannot fit the PF emission theory very well and the nonlinear dependence of ln (I/V) versus $V^{0.5}$ eliminates the possibility of PF emission. With consideration that the sulfide-treated CdS film had a low trap density, the TE-diffusion may be the possible phenomenon that explains the deviation from the ideality of the PEDOT:PSS:ZnO/sulfide-treated CdS/ITO device. Zhou *et al*. suggested that the dominant transport property at the

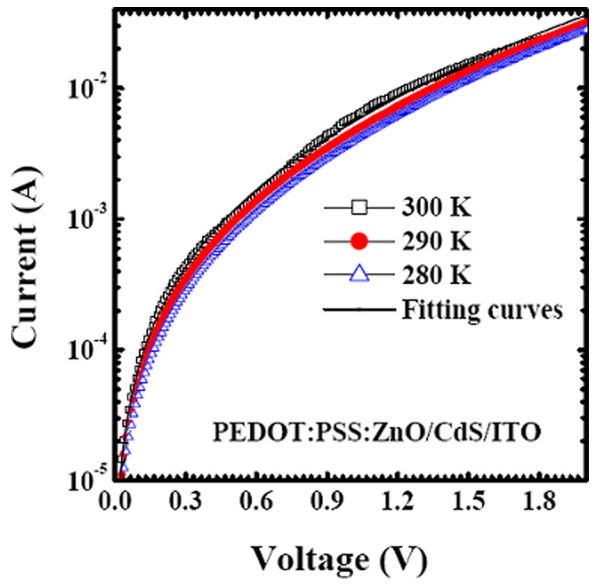

FIG. 2. The experimental results (observed at 280, 290, and 300 K) fit the Poole-Frenkel emission theory very well for PEDOT:PSS:ZnO/CdS/ITO devices.

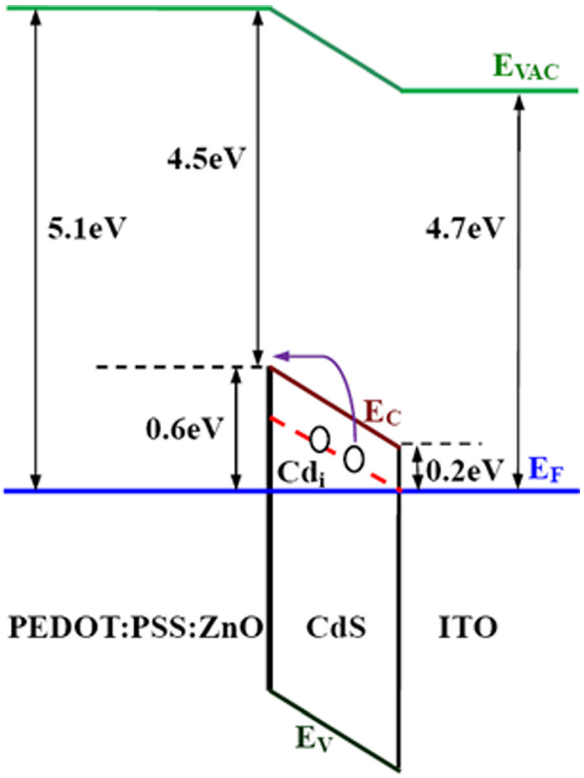

FIG. 3. Energy band diagram of PEDOT:PSS:ZnO/CdS/ITO heterojunction: the dominant transport property is the Poole-Frenkel emission, E_V is the valence-band edge, E_F is the Fermi energy level, and E_{VAC} is the vacuum level.

barrier is TE and diffusion for ZnO wire-based devices.[47] Based on the TE-diffusion theory (for $V \gg 3kT/q$), the I–V relationship is given as follows:[47]

$$I = S_a A^* T^2 \exp\left[\frac{-q\left(\phi_B - \sqrt{\frac{q\xi}{4\pi\varepsilon_r\varepsilon_o}}\right)}{kT}\right], \tag{3}$$

$$\xi = \sqrt{\frac{2qN_D}{\varepsilon_r\varepsilon_o}\left(V + V_{bi} - \frac{kT}{q}\right)}, \tag{4}$$

where A^* is the effective Richardson constant, V_{bi} is the build-in potential at the barrier, N_D is the donor impurity density, and $q\phi_B$ is the barrier height. This model can be distinguished via the linear ln (I)-$V^{0.25}$ correlation. It is found that the ln (I)-$V^{0.25}$ curve (Fig. 4) of PEDOT:PSS:ZnO/sulfide-treated CdS/ITO devices is very linear, which is consistent with Eq. (3). This indicates that the TE-diffusion model is the dominant process in our PEDOT:PSS:ZnO/sulfide-treated CdS/ITO device. We deduce that the sulfide treatment leads to a reduction in the number of Cd_i, which leads to the conversion of carrier transport behavior. In addition, a shift of the fitting line (Fig. 4) is attributed to a change in $q\phi_B$.

To confirm the presence of defects in the CdS films and to verify the effect of defects, the PL spectra were obtained for CdS samples. Luminescence is the most common characteristic that demonstrates the energy structure and defects of these thin films. Figure 5(a) shows the PL spectra of CdS

Reuse of AIP Publishing content is subject to the terms at: https://publishing.aip.org/authors/rights-and-permissions. Download to IP: 91.202.128.12 On: Thu, 23 Jun 2016 05:14:59

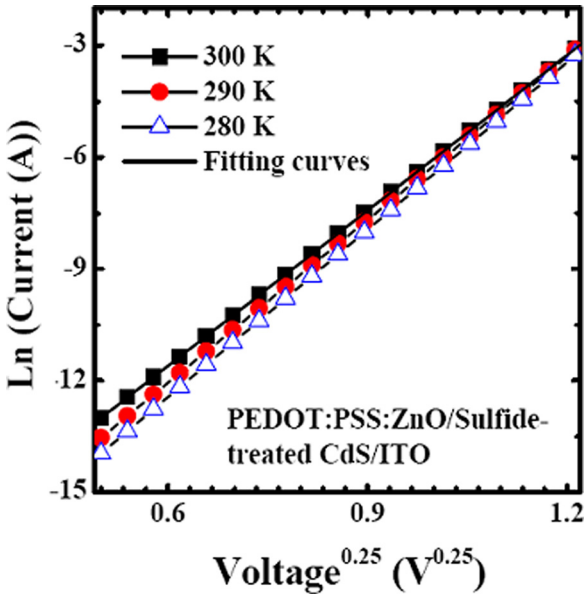

FIG. 4. The experimental results (observed at 280, 290, and 300 K) fit the thermionic emission-diffusion theory very well for PEDOT:PSS:ZnO/sulfide-treated CdS/ITO devices.

samples without sulfide treatment. There are seven emission peaks (peak positions at 2.45, 2.21, 2.11, 2.00, 1.83, 1.69, or 1.55 eV) are noted.[5,41,48–52] Three types of point defects, which can be present in CdS generating three trap levels inside the energy gap, were identified.[41,48–52] The vacancies in cadmium and sulfur are treated as localized acceptor and donor states, but Cd_i is the donor state. The peak at 2.45 eV is the band-gap edge luminescence.[5,48] The peak at 2.11 or 2.21 eV is attributed to the Cd_i-related emission.[49,50] The PL peak observed at 2.00 or 1.55 eV is caused by a donor-acceptor pair.[40,49] The peaks at 1.83 and 1.69 eV are attributed to the V_S-related emission.[48,52] Figure 5(b) shows the PL spectra of CdS sample without (with) sulfide treatment based on the normalized 2.45-eV peak intensity. Depending on sulfide treatment, an evolution and improvement of the PL signal were observed. It is found that sulfide treatment leads to a reduced intensity for the V_S-related luminescence. Simultaneously, sulfide treatment leads to a reduced intensity for the Cd_i-related luminescence. It is suggested that the number of Cd_i is reduced as the number of V_S is reduced. Abken *et al*. suggested that the loss in sulfur may induce additional Cd_i defect levels.[41] A positive example has demonstrated that through preparing CdS films in a sulfur-enrichment atmosphere, the trap states introduced by V_S or Cd_i could be significantly reduced.[43,53,54] This observation can be attributed to the fact that the adsorption (incorporation) of the sulfur atoms during the sulfide treatment process leads to an increased probability of the formation of V_S occupied by S that serves to promote the formation of Cd-S bonds, which leads to a reduction in the number of Cd_i in the CdS films.

Figure 6 shows the AFM images of CdS films with (without) sulfide treatment. It is found that the value of the root-mean-square surface roughness is 2.61 (1.56) nm for CdS samples without (with) sulfide treatment. This implies that sulfide treatment produces a smoother CdS surface. In order to obtain a greater understanding of the reduction in the number of defects in the CdS films, the photoelectrochemical measurement was performed. The photocurrent density of the CdS/ITO electrode as a function of applied voltage is shown in Fig. 7. For CdS samples with sulfide treatment, the increase in the photocurrent density is the result of the adsorption (incorporation) of sulfur atoms during the sulfide treatment process that serves to reduce the number of donor-like defects in the CdS films. The increase in the photocurrent density has been ascribed to a combination of several factors including the reduction in the recombination of photogenerated electrons with redox ions, removal of surface contaminants, change in surface physical structure, and modification of surface chemical structure causing change in surface energetics.[55,56] In addition, the

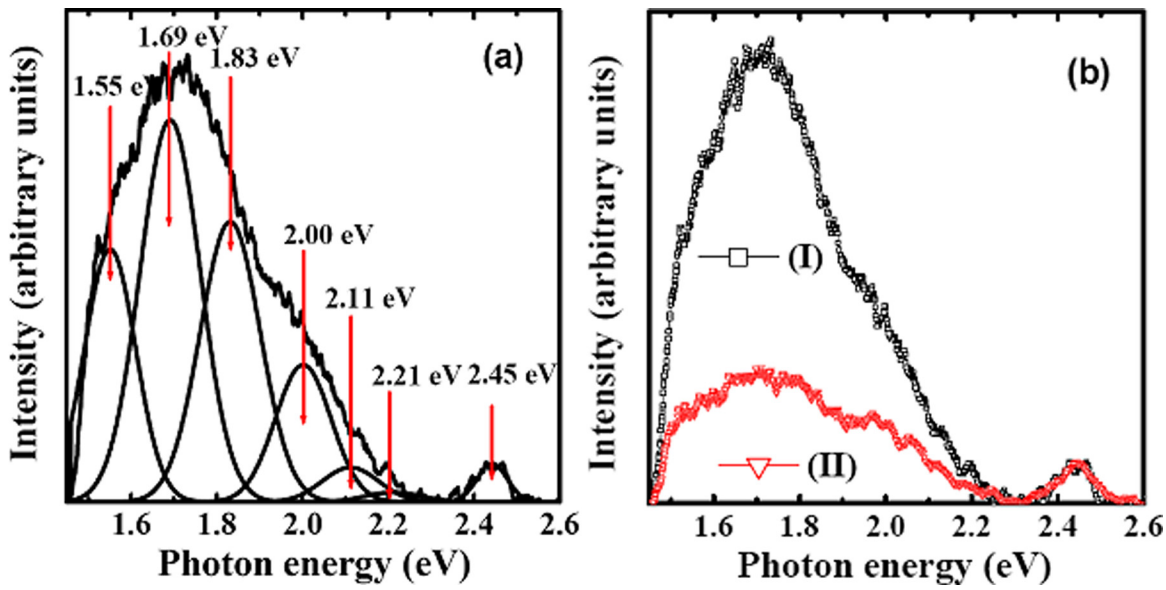

FIG. 5. (a) The PL spectra of CdS samples without sulfide treatment and (b) the PL spectra of CdS samples (I) without and (II) with sulfide treatment.

Reuse of AIP Publishing content is subject to the terms at: https://publishing.aip.org/authors/rights-and-permissions. Download to IP: 91.202.128.12 On: Thu, 23 Jun 2016 05:14:59

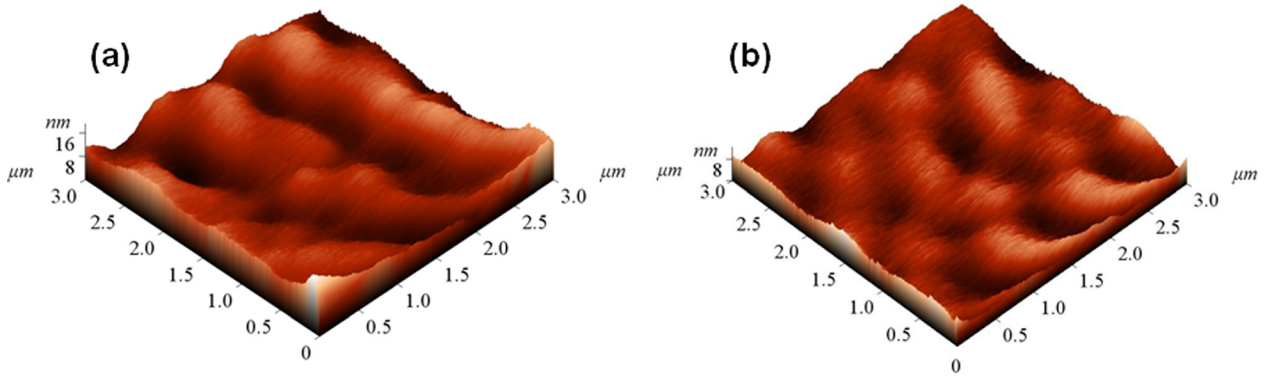

FIG. 6. The AFM images of CdS samples (a) without and (b) with sulfide treatment.

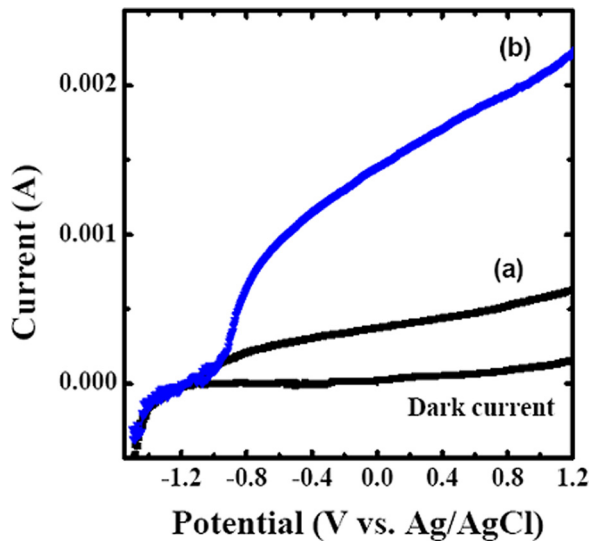

FIG. 7. Variation of photocurrent versus measured potential for CdS/ITO working electrodes (a) without and (b) with sulfide treatment.

photoconversion efficiency (E_p) of light to chemical energy in the presence of an external applied potential has been defined.[57] For CdS samples with (without) sulfide treatment, E_p was calculated to be 2.0 (0.5)%. The PL and photoconversion results imply that an increase in the value of E_p is the result of a reduction in the number of donor-like defects (that is, Cd_i and V_S).

IV. CONCLUSION

The defect-dependent carrier transport behavior of PEDOT:PSS:ZnO/CdS/ITO devices was investigated in this study. It is found that the carrier transport behavior is governed by the PF emission for PEDOT:PSS:ZnO/CdS/ITO devices. However, the carrier transport behavior is governed by the TE-diffusion for PEDOT:PSS:ZnO/sulfide-treated CdS/ITO devices. In order to understand this phenomenon and to determine the correlation between the electrical properties and defects, the photoluminescence and photoelectrochemical measurements were performed. It is shown that sulfide treatment leads to a reduction in the number of donor-like defects (that is, Cd_i and V_S) in the CdS films, which leads to the conversion of carrier transport behavior for PEDOT:PSS:ZnO/CdS/ITO devices.

ACKNOWLEDGMENTS

The authors acknowledge the support of the Ministry of Science and Technology, Taiwan (Contract Nos. 103-2112-M-018-003-MY3 and 100-2112-M-018-003-MY3) in the form of grants.

[1]K. S. Ramaiah and A. K. Bhatnagar, J. Mater. Sci. - Mater. Electron. **11**, 269 (2000).
[2]S. J. Lade and C. D. Lokhande, Mater. Chem. Phys. **49**, 160 (1999).
[3]G. Pérez-Hernández, J. Pantoja-Enríquez, B. Escobar-Morales, D. Martinez-Hernández, L. L. Díaz-Flores, C. Ricardez-Jiménez, N. R. Mathews, and X. Mathew, Thin Solid Films **535**, 154 (2013).
[4]H. K. Seo, E. A. Ok, W. M. Kim, J. K. Park, T. Y. Seong, D. W. Lee, H. Y. Cho, and J. Jeong, Thin Solid Films **546**, 289 (2013).
[5]G. Murali, D. A. Reddy, S. Sambasivam, G. Giribabu, R. P. Vijayalakshmi, R. Venugopal, and B. K. Reddy, Mater. Lett. **93**, 149 (2013).
[6]J. H. Schon, O. Schenker, and B. Batlogg, Thin Solid Films **385**, 271 (2001).
[7]M. Rami, E. Benamar, M. Fahoume, and A. Ennaoui, Phys. Status Solidi A **172**, 137 (1999).
[8]A. Zyoud, I. Saa'deddin, S. Khudruj, Z. M. Hawash, D. Park, G. Campet, and H. S. Hilal, Solid State Sci. **18**, 83 (2013).
[9]M. A. Islam, M. S. Hossain, M. M. Aliyu, P. Chelvanathan, Q. Huda, M. R. Karim, K. Sopian, and N. Amin, Energy Procedia **33**, 203 (2013).
[10]B. Ullrich, D. Ariza-Flores, and M. Bhowmick, Thin Solid Films **558**, 24 (2014).
[11]S. A. Jassim, A. A. R. A. Zumaila, and G. A. A. A. Waly, Results Phys. **3**, 173 (2013).
[12]H. Y. Tsao and Y. J. Lin, Appl. Phys. Lett. **104**, 053501 (2014).
[13]Y. J. Lin and Y. M. Chin, Appl. Phys. Lett. **103**, 173301 (2013).
[14]J. H. Lin, J. J. Zeng, Y. C. Su, and Y. J. Lin, Appl. Phys. Lett. **100**, 153509 (2012).
[15]Y. J. Lin and Y. C. Su, J. Appl. Phys. **111**, 073712 (2012).
[16]Y. J. Lin and Y. M. Chin, J. Appl. Phys. **116**, 173709 (2014).
[17]D. Lincot, Thin Solid Films **487**, 40 (2005).
[18]C. F. You, Y. J. Lin, C. J. Liu, and C. A. Wu, J. Lumin. **146**, 109 (2014).
[19]B. M. Basol, Sol. Cells **23**, 69 (1988).
[20]S. K. Das and G. C. Morris, J. Appl. Phys. **73**, 782 (1993).
[21]N. Maticiuc, J. Hiie, T. Raadik, A. Graf, and A. Gavrilov, Thin Solid Films **535**, 184 (2013).
[22]R. K. Sharma, S. N. Sharma, and A. C. Rastogi, Curr. Appl. Phys. **3**, 257 (2003).
[23]J. A. Hernández, J. S. Hernández, R. M. Pérez, M. C. García, and G. C. Puente, Phys. Status Solidi C **2**, 3710 (2005).
[24]J. H. Lee and D. J. Lee, Thin Solid Films **515**, 6055 (2007).
[25]Y. J. Lin, C. F. You, H. C. Chang, C. J. Liu, and C. A. Wu, J. Lumin. **158**, 407 (2015).

Reuse of AIP Publishing content is subject to the terms at: https://publishing.aip.org/authors/rights-and-permissions. Download to IP: 91.202.128.12 On: Thu, 23 Jun 2016 05:14:59

[26]D. A. Neamen, *Semiconductor Physics and Devices: Basic Principles*, 3rd ed. (McGraw-Hill, Boston, 2003).
[27]D. K. Schroder, *Semiconductor Material and Device Characterization*, 3rd ed. (John Wiley & Sons, New Jersey, 2006).
[28]S. Sönmezoğlu, Appl. Phys. Express **4**, 104104 (2011).
[29]S. Sönmezoğlu, S. Şenkul, R. Taş, G. Çankaya, and M. Can, Solid State Sci. **12**, 706–711 (2010).
[30]S. Sönmezoğlu, Ö. A. Sönmezoğlu, G. Çankaya, A. Yıldırım, and N. Serin, J. Appl. Phys. **107**, 124518 (2010).
[31]C. He, C. B. Han, Y. R. Xu, and X. J. Li, J. Appl. Phys. **110**, 094316 (2011).
[32]H. J. Xu and X. J. Li, Appl. Phys. Lett. **93**, 172105 (2008).
[33]Y. P. Gong, A. D. Li, X. Qian, C. Zhao, and D. Wu, J. Phys. D: Appl. Phys. **42**, 015405 (2009).
[34]K. Y. Cheong, J. H. Moon, H. J. Kim, W. Bahng, and N. K. Kim, J. Appl. Phys. **103**, 084113 (2008).
[35]R. Das and S. Pandey, Int. J. Mater. Sci. **1**, 35 (2011), available at http://www.ij-ms.org/paperInfo.aspx?ID=4930.
[36]D. R. Lide, *Handbook of Chemistry and Physics*, 87 ed. (CRC Press, Boca Raton, FL, 1998), pp. 4–67, 1363. ISBN 0-8493-0594-2.
[37]S. Malik, A. K. Ray, A. K. Hassan, and A. V. Nabok, IEEE Trans. Nanotechnol. **2**, 149 (2003).
[38]K. I. Kirov, Phys. Status Solidi B **39**, 531 (1970).
[39]A. Veamatahau, B. Jiang, T. Seifert, S. Makuta, K. Latham, M. Kanehara, T. Teranishid, and Y. Tachibana, Phys. Chem. Chem. Phys. **17**, 2850 (2015).
[40]J. J. Ramsden, S. E. Webber, and M. Grätzel, J. Phys. Chem. **89**, 2740 (1985).
[41]A. E. Abken, D. P. Halliday, and K. Durose, J. Appl. Phys. **105**, 064515 (2009).
[42]S. Senthilarasu, R. Sathyamoorthy, S. H. Lee, and S. Velumani, Vacuum **84**, 1212 (2010).
[43]Y. Li, L. L. Wang, X. B. Wang, L. L. Yan, L. X. Su, Y. T. Tian, and X. J. Li, Chin. Phys. B **23**, 087307 (2014).
[44]A. M. Nardes, M. Kemerink, M. M. de Kok, E. Vinken, K. Maturova, and R. A. J. Janssen, Org. Electron. **9**, 727 (2008).
[45]K. H. Lee, H. W. Jang, K. B. Kim, Y. H. Tak, and J. L. Lee, J. Appl. Phys. **95**, 586 (2004).
[46]J. Lee, W. Lee, T. Park, J. Lee, E. Park, D. Lee, J. Lee, and W. Yi, J. Vac. Sci. Technol., B **28**, C2B43 (2010).
[47]J. Zhou, P. Fei, Y. Gu, W. Mai, Y. Gao, R. Yang, G. Bao, and Z. L. Wang, Nano Lett. **8**, 3973 (2008).
[48]O. Vigil, I. Riech, M. G. Rocha, and O. Z. Angel, J. Vac. Sci. Technol., A **15**, 2282 (1997).
[49]H. A. Calderon, R. L. Morales, O. Z. Angel, J. G. M. Alvarez, and L. Baños, J. Vac. Sci. Technol., A **14**, 2480 (1996).
[50]R. L. Morales and O. Z. Angel, Thin Solid Films **281–282**, 386 (1996).
[51]L. Wan, Z. Bai, Z. Hou, D. Wang, H. Sun, and L. Xiong, Thin Solid Films **518**, 6858 (2010).
[52]Y. Shiraki, T. Shimada, and K. F. Komatsubara, J. Appl. Phys. **45**, 3554 (1974).
[53]R. Mendoza-Pérez, J. Aguilar-Hernández, J. Sastre-Hernández, N. Ximello-Quiebras, G. Contreras-Puente, G. Santana-Rodríuez, O. Vigil-Galán, E. Moreno-García, and A. Morales-Acevedo, Sol. Energy **80**, 682 (2006).
[54]J. Aguilar-Hernández, J. Sastre-Hernández, N. Ximello-Quiebras, R. Mendoza-Pérez, O. Vigil-Galán, G. Contreras-Puente, and M. Cárdenas-García, Thin Solid Films **511–512**, 143 (2006).
[55]R. Sharma, P. P. Das, M. Misra, V. Mahajan, J. P. Bock, S. Trigwell, A. S. Biris, and M. K. Mazumder, Nanotechnology **20**, 075704 (2009).
[56]C. Chen, L. Wang, F. Li, and L. Ling, Mater. Chem. Phys. **146**, 531 (2014).
[57]C. Y. Chiang, K. Aroh, N. Franson, V. R. Satsangi, S. Dass, and S. Ehrman, Int. J. Hydrogen Energy **36**, 15519 (2011).

Reuse of AIP Publishing content is subject to the terms at: https://publishing.aip.org/authors/rights-and-permissions. Download to IP: 91.202.128.12 On: Thu, 23 Jun 2016 05:14:59